J. Embryol. exp. Morph. **96**, 19–49 (1986)
Printed in Great Britain © *The Company of Biologists Limited 1986*

Neurulation and the cortical tractor model for epithelial folding

ANTONE G. JACOBSON[1], GEORGE F. OSTER[2], GARRETT M. ODELL[3] AND LOUIS Y. CHENG[4]

[1]*Center for Developmental Biology, and Department of Zoology, University of Texas, Austin, TX 78712, USA*

[2]*Departments of Biophysics and Entomology, University of California, Berkeley, CA 94720, USA*

[3]*Department of Mathematical Sciences, Rensselaer Polytechnic Institute, Troy, NY 12181, USA.*

[4]*Department of Civil Engineering, University of California, Berkeley, CA 94720, USA*

SUMMARY

We present here a new model for epithelial morphogenesis, which we call the 'cortical tractor model'. This model assumes that the motile activities of epithelial cells are similar to those of mesenchymal cells, with the added constraint that the cells in an epithelial sheet remain attached at their apical circumference. In particular, we assert that there is a time-averaged motion of cortical cytoplasm which flows from the basal and lateral surfaces to the apical region. This cortical flow carries with it membrane and adhesive structures that are inserted basally and resorbed apically. Thus the apical seal that characterizes epithelial sheets is a dynamic structure: it is continuously created by the cortical flow which piles up components near where they are recycled in the apical region. By use of mechanical analyses and computer simulations we demonstrate that the cortical tractor motion can reproduce a variety of epithelial motions, including columnarization (placode formation), invagination and rolling. It also provides a mechanism for driving active cell rearrangements within an epithelial sheet, while maintaining the integrity of the apical seal. Active repacking of epithelial cells appears to drive a number of morphogenetic processes. Neurulation in amphibians provides an example of a process in which all four of the above morphogenetic movements appear to play a role. Here we reexamine the process of neurulation in amphibians in light of the cortical tractor model, and find that it provides an integrated view of this important morphogenetic process.

INTRODUCTION

In this paper we propose a novel mechanism for epithelial morphogenesis, which we call the 'cortical tractor' (Jacobson, Odell & Oster, 1985). This model resolves several paradoxical features of epithelial sheets, including the ability of epithelial cells to change their positions relative to their neighbours without

Key words: neurulation, modelling, epithelial folding, cortical tractor.

breaking the apical seal, and the ability of epithelial sheets to fold and invaginate in a coordinated fashion over large areas.

During early embryogenesis cell types may be classified into two general groups: mesenchyme and epithelia (Hay, 1968). Epithelial cells are organized into cohesive sheets that cover surfaces and line cavities. Each epithelial cell has a definite polarity, with the apical surface facing the external medium or the internal cavity. Just beneath the apical surface a circumferential complex of junctions bonds the epithelial cells tightly to one another and seals the embryo from the outside environment, or from the contents of the cavities. The basal surface usually faces a basal lamina and other extracellular matrix material. When epithelial cells change shape, the sheet in which they are embedded may roll, fold, invaginate or otherwise deform while retaining its integrity as a connected tissue.

Mesenchymal cells are loose, migratory cells that frequently move about beneath and between epithelial layers. The polarity of mesenchymal cells reflects their current direction of movement, which changes as the cells move about. Their migratory motions often appear relatively independent of one another, but they frequently aggregate to form patterned clusters of cells.

Embryonic morphogenesis results from the coordinated behaviour of epithelial sheets and groups of mesenchymal cells. However, the identity of these two cell types is not immutable; frequently during early embryogenesis cells convert between epithelial and mesenchymal forms (Hay, 1968). For example, epithelial cells in the epiblast of bird embryos converge to the primitive streak, pass through and detach from the epithelium to wander beneath as mesenchyme cells. Some of these form orderly clusters of cells (somitomeres) that eventually condense into epithelial somites (Meier, 1984). Later, cells in regions of the epithelial somites emerge again as mesenchyme, which then migrate and cluster to form bones, skin, or muscle masses.

Clearly, the same cytoskeletal machinery used by mesenchyme cells to move about is present in epithelial cells, albeit organized differently. We shall propose that epithelial cells do indeed move about in much the same fashion as mesenchymal cells, changing neighbours and deforming the epithelial sheet while maintaining, indeed constructing, the apical seal. The mechanism by which movement and morphogenesis are accomplished we call the *cortical tractor*; we propose it as the driving force underlying epithelial morphogenesis, including epiboly, gastrulation, neurulation, placode invagination and evagination. Here we shall apply the cortical tractor concept to explain certain paradoxical features of amphibian neurulation.

GENERAL FEATURES OF CELL MOTIONS

Motility, the capacity to move and change shape, is a fundamental property of cells, and all cells in the embryo are potentially motile. Mesenchymal cells regularly move about, and epithelial cells, when disaggregated, also move about much like mesenchymal cells (Holtfreter, 1946; Middleton, 1973). Cells at and

near the free edges of an epithelial sheet are motile, and their activities may expand the sheet (Vaughn & Trinkaus, 1966). Examples of this are the expansion of the chick blastoderm (New, 1959; Downie & Pegrum, 1971), and wound healing (Radice, 1980*a*,*b*). Epithelial cells may also move about amongst one another tangentially within an intact epithelial sheet. These movements may be organized so as to produce specific deformations of the sheet. This is a particularly paradoxical phenomenon, and one to which the cortical tractor model proposes a solution.

While there are differences in the details of how different cell types move (Trinkaus, 1984*a*), there are fundamental similarities. Oster (1984) has proposed a model for lamellipodial motion that ties together many properties of moving cells. In this model, the cell's movement is driven by the actomyosin cortical gel, which undergoes a cycle of events involving solation and osmotic expansion followed by regellation and contraction. As these events proceed, there is a fountainoid flow of cytoplasm from the cell interior to the region where the cell's anterior is protruding, and a flow of the cortex away from that region. Elsewhere in the cell the cortical material is again recycled into the cell's interior. Osmotic expansion of the partially solated gel at the lamellipod tip, together with hydrostatic pressure created by contraction of the cortical gel elsewhere, extends the tip of the lamellipod. Cell and substrate adhesion molecules are carried by the fountainoid of cytoplasm to the cell surface at the tip of the lamellipod and inserted into the membrane. These molecules adhere to adjacent cells, or to the substrate, and are attached through the membrane to the cytoskeleton of the cortex where they anchor the newly extended lamellipod tip. Thus when the cortical actin regels and commences active contraction, the cell inches forward. In this model, the tip of the lammellipod is a special site for ionic leaks that lead to an increase in free calcium in the tip cortex; it is this elevated cortical calcium concentration that initiates and maintains the solation–contraction cycle just described.

While the details of this particular model may not apply to all cells (or even to any cells), what is crucial to our discussion are the following features of cell motion: (a) the overall flow pattern of cytoplasm, and (b) the insertion of adhesion molecules in the leading edge. In the following section we will extract these properties and formalize them as a set of postulates that embody the cortical tractor model.

THE CORTICAL TRACTOR MODEL

The cortex of a moving cell flows in a fountainoid pattern

The cortical tractor model will apply to all motile cells, whether crawling as individuals or in groups; in particular, it will apply to cells joined into an epithelial sheet. The first postulate of the cortical tractor model is:

> *Cell motion is characterized by a 'fountainoid' flow pattern of cytoplasm from the leading to the trailing edge of the crawling cell, as shown in Fig. 1. We shall call this flow pattern the 'cortical tractor'.*

Several authors have suggested, and given evidence for, this type of cortical motion (e.g. Allen, 1961; Abercrombie, Heaysman & Pegrum, 1970; Harris, 1973; Odell & Frisch, 1975; Abercrombie, 1980; Dembo & Harris, 1981; Bretscher, 1984). Abercrombie *et al.* (1970), Harris & Dunn (1972) and Dembo & Harris (1981), among others, did marking experiments that demonstrated that the cortical flow is reflected on the surface of the cell, indicating an intimate connection between the flowing cortex and the plasma membrane. Bretscher (1984) focuses on the flow of the membrane and its return to the interior *via* endocytotic vesicles. He suggests that the motion of the cell is the result of membrane flow; however, since the plasma membrane is fluid, it does not have the mechanical properties necessary for cell movement (see, for example, the discussion by Ambrose after the paper by Petris & Raff, 1973).

In our model, the essential feature is the flow pattern of the cortical gel. The membrane may or may not follow the cortical flow; its essential role in the setting of the model is to regulate the communication between the cell and its ionic environment. Also, a particular cell may generate more than one tractoring locus; indeed, any motile region of a cell's cortex will undergo local tractoring in a pattern analogous to that shown in Fig. 1.

Adhesion structures are cycled with the cortical flow

In order for the cortical tractor to drive cell movement there must be adhesion structures anchoring the cell to its substrate or to neighbouring cells. The cortical tractor model requires that these adhesive molecules are cycled along with the cortex (Campbell & Campbell, 1971). Therefore, our second postulate is:

Adhesion and junctional molecules are inserted at the site of the cortical 'source' (the cell's leading surface). They flow posteriorly with the cortex and are resorbed at the cortical 'sink', unless stabilized by bonding with the substratum, or with another cell.

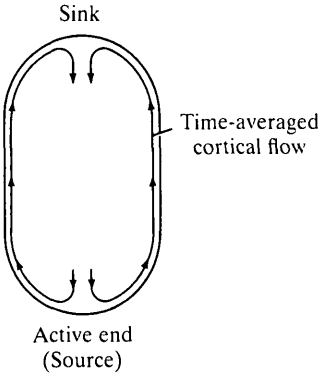

Fig. 1. Schematic of the cortical tractor mechanism. The actomyosin cortex has a time-averaged flow as indicated by the arrows, and the cell-to-cell adhesion structures are dragged along by the flow of the cortex.

A moving cell attaches itself to its substratum by attachment sites that are continuously being inserted at the leading edge. These sites are dragged towards the cell's posterior where they are resorbed. Cell–cell and cell–substrate adhesion sites pass through the membrane, attaching the cell's cortex to the point of adhesion outside the cell. Being a lipid fluid, the membrane can flow around the attachment sites, or alternatively the sites may be dragged through the fluid membrane. Junctional structures inserted at the leading edge of the cell flow with the cortex to the trailing edge, where they may become a transient part of specific junctions, such as desmosomes (Campbell & Campbell, 1971).

Ionic stimuli may activate the cortical tractor

The cortical tractor may be activated by ionic stimuli. Experiments with ionophores and channel-plugging molecules show that cell motility can be stimulated by ionic leaks, especially of calcium, and inhibited by blocking ionic channels (Zigmond, 1978; Snyderman & Goetzl, 1981; Cooper & Schliwa, 1985). Anything that initiates ionic leaks at a cell surface (or blocks such leaks) could start (or stop) cell movement in that direction. The direction of movement (i.e. the orientation of the cortical source) is an important part of the cortical tractor model. There is ample evidence for cellular and molecular mechanisms that regulate ionic conditions, although it is not yet clear how they are mediated. The proximal signal for activating the surface of a cell could be nonionic chemical messengers such as chemotactic agents that bind specific receptors on the cell surface and initiate ionic events that trigger motile activity. A variety of mechanisms and components may regulate calcium and other ions that affect motility (Hitchcock, 1977; Oster, 1984). We need not be specific about these mechanisms here, for whatever the details may be, the only essential aspect for the cortical tractor model is that motility can be triggered by the local chemical environment.

Epithelial cells remain attached to one another at their apical ends

The final ingredient of the cortical tractor model of epithelial morphogenesis requires that epithelial cells have some mechanism of maintaining their integrity as a cell sheet. Thus our third postulate is:

> *Cortical tractoring occurs in epithelial cells much as it does in mesenchymal cells, except that epithelial cells remain firmly attached to one another at their apical boundaries.*

The cortical tractor suggests a mechanism for this attachment: if the recycling rate for adhesion structures is slower than their insertion at the cortical source (i.e. the basal surface), then they will 'pile up' at the apical end, and prevent the cells from detaching.

Epithelial sheets are dynamic structures

The cortical tractor model views an epithelial sheet not as a static cobblestone paving of cells, but as a dynamic structure that is in constant motion. As shown in

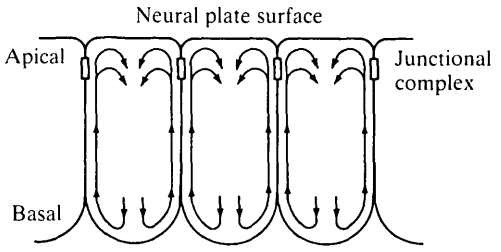

Fig. 2. Schematic of a cross section of an epithelial sheet. The time-averaged flow of the cortex in each cell comprises the cortical tractor motion (arrows). This cortical flow inserts adhesive structures at the basal source, and reabsorbs them in the apical region. These junctional molecules pile up at the apical end and form the apical seal, a structure that is constantly being renewed. As long as the time-averaged speed of the cortical tractor in adjacent cells remains approximately equal, no shear forces will be generated, and no deformation of the epithelial sheet will take place.

Fig. 2, each cell is constantly tractoring its cortex from basal (or basolateral) to apical, and the apical seal is continuously renewed by the insertion and recycling of adhesive structures (e.g. Larsen & Risinger, 1985). As we mentioned earlier, there is evidence that suggests that more than one tractor site can coexist on a given cell. For example, different virus particles will insert specifically at basal, lateral or apical surfaces of an epithelial cell, and exocrine cells secrete through their apical surfaces; therefore, there can be a basal, apical and, or, lateral tractor operating at various times in a cell. Therefore, the time-averaged flow of cortical cytoplasm is likely to be more complicated than a simple basal-to-apical motion; however, many of the phenomena we shall discuss can be understood in terms of the simplified cortical flow shown in Fig. 2.

Differences in cortical tractor velocity will deform an epithelial sheet

The apical surface of an epithelial cell does not become an active, leading edge except in unusual circumstances, and then the cell is likely to crawl out of the epithelium (cf. Holtfreter, 1947). However, any other free surface of the cell, either basal or lateral, or both, may be active. Each cell in Fig. 2 is attempting to crawl downward on its neighbours by adhesion to their surfaces and contraction of its cortex. *However, if adjacent cells are equally active in their crawling motions, no net traction can be developed between them, and no net motion results.* If the intensity of crawling (i.e. the speed of the cortical tractor) is different between adjacent cells, shear forces will be generated and the faster cell will commence to crawl basalward, out of the sheet. The apical junctional complexes restrain each cell from detaching from the epithelial sheet, and so the net effect of differential crawling is that cells crawling most rapidly elongate in the basal direction. Thus imposing a gradient of tractor velocity will convert cuboidal epithelial cells into a columnar morphology.

Of course, a verbal statement of such a course of events cannot be convincing, and so we have constructed a mechanical model to demonstrate how an epithelium consisting of cuboidal cells can generate placode regions of columnar cells by

differences in the speed of the cortical tractor (Cheng, Murray, Odell & Oster, 1986; a sketch of this model is given in Appendix A).

Epithelial morphogenesis is driven by cell shape change

An epithelial layer as a whole can deform by spreading, retracting, folding, bending, rolling into a tube, evaginating or invaginating. As such deformations proceed, the constituent cells of the epithelium change shape. Indeed, it is fair to assume that the global deformations of the sheet are driven by the shape changes of the individual cells. In order to change its shape, an epithelial cell must generate internal forces to work against the tractions of its neighbouring cells. Bundles of microfilaments are often found encircling the apical surface of cells in a deforming epithelium, and the constriction of these filament bundles is thought to contract the apical surfaces to create wedge-shaped cells which would roll the epithelial sheet (Baker & Schroeder, 1967; Burnside, 1971; Odell, Oster, Alberch & Burnside, 1981).

The cortical tractor mechanism dramatically augments the apical filament bundle hypothesis by providing an additional means by which epithelial cells can change shape. Indeed, the cytoplasmic flow pattern associated with the cortical tractor mechanism suggests that the microfilaments may have accumulated in the apices by the tractor motion. Moreover, the cortical tractor mechanism can reproduce all of the epithelial foldings associated with the apical contraction model (Odell *et al.* 1981) as well as many deformations that apical contraction alone cannot produce. (For example, the cuboidal-to-columnar transitions characterizing placode formation which precede most foldings cannot easily be generated by apical contractions.)

Epithelial cells can change neighbours without breaking the apical seal

One of the most paradoxical properties of cells in an epithelium is their ability to move within the plane of the sheet, thereby changing their neighbour relationships, without violating the integrity of the apical seal. For example, neighbour changes are frequently seen in apical views of the midline of the neural plate (Jacobson & Gordon, 1976), and in the surface epithelium near the blastopore during amphibian gastrulation (Keller, 1978). Such cell rearrangements have also been seen in the epithelia of insect imaginal discs (Fristrom, 1982) and in the enveloping layer of *Fundulus* (Trinkaus, 1984*b*).

The general situation is shown in Fig. 3A: cells *b* and *d* do not contact one another initially, but at a later time they come to share a common boundary. Any kind of epithelial rearrangement can be built up from such binary neighbour changes. The cortical tractor mechanism suggests that the answer to such apical reorganizations lies below the surface, as shown in Fig. 3B. Cell *b* becomes active on its lateral face and puts out a protrusion toward cell *d*. As the lamella is carried apicalward by the cortical flow, it eventually appears from above as a cytoplasmic extension extruding itself between cells *a* and *c*. That is, an apical view would give

the impression that *b* had crawled between *a* and *c*, and so must have broken their apical bonds. However, this is an illusion, for no bonds need be broken. Rather the flow of new adhesive and junctional structures up from below replaces the junctions being recycled to the interior of the cells. Thus the apical seal is never broken, as the cells actively interdigitate between one another.

Cell repacking may drive other morphogenetic processes

There is a growing body of observations that support the conclusion that epithelial sheets can alter their global geometry by an active repacking of their constituent cells. This may underlie such diverse phenomena as the evagination of imaginal discs in *Drosophila* (Fristrom, 1982), and late gastrulation in sea urchins (Ettensohn, 1985; Harding & Cheng, 1986). Indeed, epiboly (the spreading and flattening of an epithelial sheet) generally involves cell rearrangements, although in some cases it appears as if they may be passively driven by forces developed at the edge of the sheet (e.g. epiboly in *Fundulus*, Trinkaus, 1984*b*). The cortical tractor mechanism provides a means for cells in an epithelial layer to repack actively, and in so doing drive large-scale changes in the geometry of the sheet. How these active repackings are coordinated so as to arrive at the desired end configuration may vary from tissue to tissue. In the next section we suggest how this coordination can be achieved during neurulation.

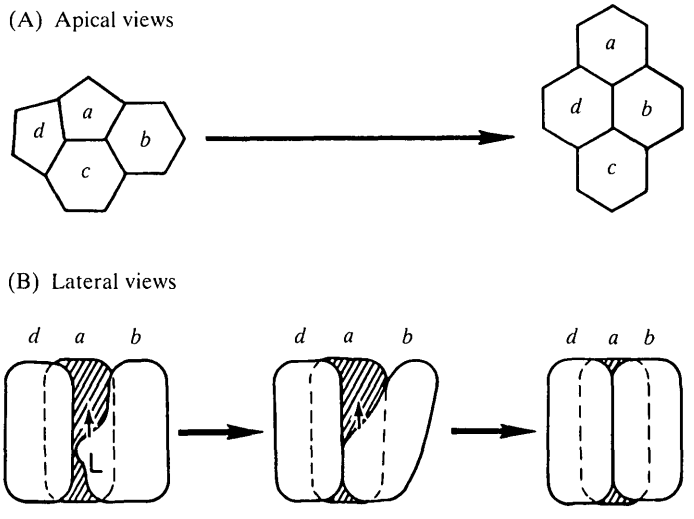

Fig. 3. (A) An apical view of four epithelial cells undergoing binary neighbour exchange. Cells *a* and *c* lose their shared apical boundary, and cells *b* and *d* come together to form a neighbour pair. (B) A lateral view of how the cortical tractor mechanism effects neighbour exchanges. Cell *b* interdigitates between cells *a* and *c* by extending lateral lamellae (L) which are swept upwards by the cortical motion. L carries with it new adhesive structures which pile up at the bottom of the apical junction, replacing ingested junctional structures. When L reaches the apical surface it appears from above as an extension of cell *b* which is interdigitating between cells *a* and *c*.

Summary of the cortical tractor model

In summary, the cortical tractor model for epithelial motility is composed of the following sequence of events.

(1) A change in the local chemical environment initiates motile activity in the basal and, or, lateral surfaces of epithelial cells, and lamellae commence to extrude from the active surfaces.

(2) The flow of cytoplasm from the interior of the cell brings adhesive and junctional structures to the cell surface at the source, where they insert through the membrane and adhere to the substratum or to adjacent cells.

(3) Cytoplasm flows into the protrusions at the active face of the motile cell, gels and contracts. This produces an average movement of cortical cytogel that flows in a fountainoid pattern (cf. Fig. 1) from basal/lateral to apical.

(4) Adhesive structures are swept by the cortical flow apicalward where they pile up and form the apical seal, eventually being resorbed into the cell interior.

(5) Adjacent cells tractoring at the same velocity cannot develop any shear forces. Therefore an epithelial sheet, whose cells are all tractoring with the same intensity, will appear as a static structure. However, if a velocity gradient develops, shear forces are generated that deform the epithelial sheet as each cell attempts to crawl out of the layer on its neighbours.

In the next section we apply these ideas to the process of neurulation, and show how boundaries between domains of different cell types act as organizing centres to coordinate the shear forces developed by the cells of the neural plate.

NEURULATION

In the embryos of amniotes and many amphibia the neural ectoderm is a simple, or single-layered, neuroepithelium. It first appears as a region of cells that columnarize, becoming taller than the rest of the ectoderm (Fig. 4).

In mammals (Jacobson & Tam, 1982) and birds (Schoenwolf, 1985), the neural plate grows during neurulation; however, amphibia are simpler to study because neurulation proceeds without growth (Jacobson, 1978). Some amphibia have very large cells with variegated egg pigmentation that makes direct observation of individual cells possible. Thus we shall use neurulation in the California newt *Taricha torosa* as a prototype of cortical-tractor-driven morphogenesis (Jacobson, 1981). Developmental stages for this species were described by Twitty & Bodenstein, and are illustrated in Rugh (1948).

During neurulation a number of morphological changes occur in the neural plate:

(1) The cells of the plate change shape, first changing from cuboidal to columnar, and finally becoming wedge-shaped.

(2) The width of the neural plate decreases, and its total surface area shrinks.

(3) The midline of the plate elongates, and cells of the notoplate undergo systematic neighbour changes.

(4) The neural folds form at the plate edges, and subsequently elongate.

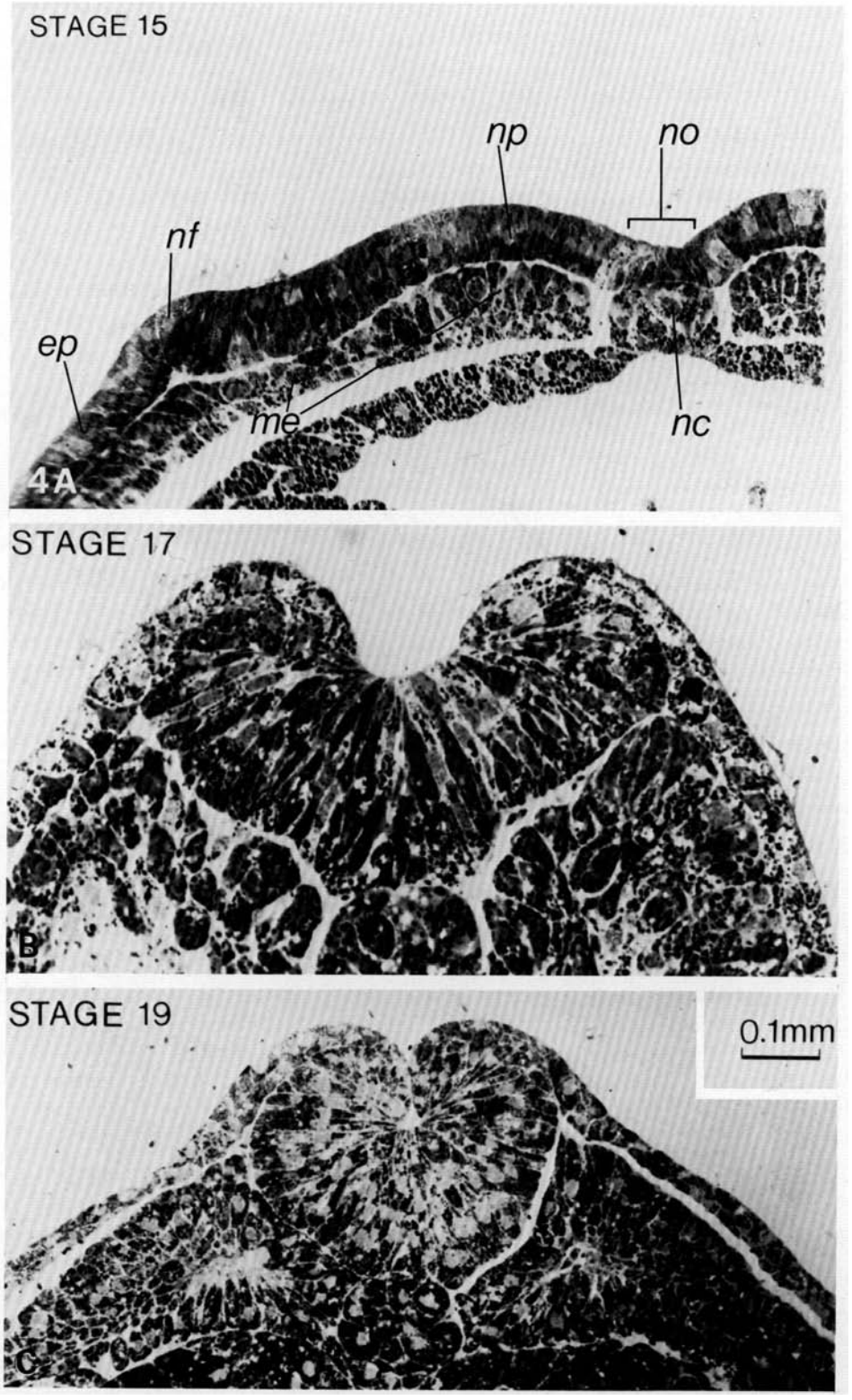

Fig. 4. The neural plate of a newt embryo, and the tissues that underlie it, are shown in cross section at stages through the period of neural fold formation and rolling of the plate into a tube. These plastic sections (2 μm thick) are from the region where the spinal cord joins the brain. All are at the same magnification. (A) Stage 15; (B) stage 17; (C) stage 19. *ep*, epidermis; *me*, mesoderm; *nc*, notochord; *nf*, neural fold; *no*, notoplate; *np*, neural plate. Bar, 0·1 mm.

(5) The plate rolls into a tube.

Each of these changes contributes to the shaping of the plate and the formation of the neural tube. In this section we shall argue that the cortical tractor is a contributing force to all of these events.

Cell shape changes accompany neurulation

The cells of the neural plate continue to get taller throughout the course of neurulation, but cells in different regions of the plate seem programmed to arrive at characteristically different heights by the end of the process (Jacobson & Gordon, 1976). The specific cell shape changes can be followed only in a mapped system because cells move long distances during neurulation. Studies that purport to describe changes in the shapes of the neural plate cells during neurulation by examining sections (e.g. Baker & Schroeder, 1967) are really describing the shapes of different groups of plate cells at different times. This is because there is a continuous flow of cells through the site of sectioning during neurulation. Burnside & Jacobson (1968) mapped the changes of cell position in the neural plate of *Taricha torosa* by analysing time-lapse films of neurulation. Burnside (1971, 1973) has correlated apical constriction of the cells to circumferentially organized purse-strings of microfilaments near the apical surface, and elongation to microtubules oriented along the long axes of the cells. She gives evidence that the apical microfilament bundles may be contracting to reduce the surface area, and that microtubules may play a role in cell elongation, perhaps by directing cytoplasmic flow toward the basal ends of the cells (Burnside, 1971).

Neural plate cells change neighbours during neurulation

Changes of cell shape, driven by apical contraction and/or the cortical tractor, play a central role in neurulation. However, certain cell groups in the neural plate appear to be more active in changing neighbours than in changing shape, and the consequences of their movements are essential for shaping the plate. Jacobson & Gordon (1976) found that the neural plate consists of two populations of cells. One group of cells overlies the notochord, and the other comprises the rest of the neural plate. We will refer to these populations as *notoplate* and *neural plate*, respectively.

Convergence and extension of notoplate is crucial in shaping the plate

In the early gastrula, the prospective notoplate is a crescent of tissue between the prospective neural plate and the prospective notochord. The notochord anlage sits on the dorsal lip of the forming blastopore (Fig. 5).

The notochord involutes around the blastopore lip, then converges toward and extends along the midline. The notoplate does not involute, but remains on the surface as part of the neural plate. It undergoes the same convergence–elongation movements as the notochord that underlies it.

The notoplate begins as a crescent of cells near the blastopore, then converges toward and elongates along the midline, a process which distorts the geometry of

the plate (Fig. 5). In an experimental study and computer simulation, Jacobson & Gordon (1976) found that the early shaping of the neural plate into a keyhole shape is largely due to the elongation of the notoplate, but also requires apical constriction of the plate cells in order for the plate shape to come out normal.

The elongation of the midline is even more dramatic during closure of the keyhole-shaped plate into a tube. During that period, elongation of the plate is ten times as fast as before or after (Jacobson & Gordon, 1976). Jacobson (1978) proposed that midline elongation of the plate could shape it into a tube by the same mechanism that rolls a rubber sheet when it is stretched along a line (so-called 'Poisson buckling').

Notoplate cells and neural plate cells are two separate populations

Besides the differences in behaviour described between notoplate and neural plate cells, there are other observations that suggest these are quite different populations of cells. For example, the notoplate cells look different from the cells of the rest of the neural plate (Fig. 6).

Keller and coworkers (Keller, Danilchik, Gimlich & Shih, 1985) explanted pieces of the dorsal lip of the blastopore of early gastrulae of the anuran *Xenopus laevis*. In culture, the explanted dorsal lip displayed four distinct regions, each with different behaviours. Prospective bottle-cells and head mesoderm from the lip of the forming blastopore continued their normal development in culture. Cells in the region of the prospective notochord underwent convergence and extension along a line, just as they would have in the embryo. A third group of cells forms the prospective notoplate, and these cells too have the intrinsic capacity to execute the convergence and elongation movements. The final region in the explant is the prospective neural plate and, in the absence of underlying inductors, these cells form a vesicle of indifferent ectoderm. It should be noted that the intrinsic behaviour of the notoplate cells does not require induction by underlying tissues.

The notoplate behaves like the notochord, except it does not involute. It may have been induced earlier along with the notochord (Gerhart, 1980). In the experiments of Spemann & Mangold (1924) that won the Nobel Prize, a piece of the dorsal lip of the blastopore of an early gastrula of *Triton cristatus* was transplanted into the ventral ectoderm of a *Triton taeniatus* host embryo. A second neural plate was induced in the ventral ectoderm of the host embryo by the implanted dorsal lip material. Differences in pigmentation between donor and host species allowed the tissues of the two species to be distinguished from one another. At least in some cases, the induced neural plate formed from host tissue, except for the midline region (i.e. the notoplate) that came from the grafted implant (Spemann, 1938, his fig. 78, p. 144). The donor notoplate cells must have insinuated themselves down the midline of the induced host neural plate. In Spemann's illustrations of sections through the spinal cord of later stages, when the secondary nervous system had formed into a tube, the donor notoplate tissue appears as the floor plate of the spinal cord (Spemann, 1938, his fig. 80, p. 146). The notoplate, in fact, maps congruent with the floor plate of the nervous system.

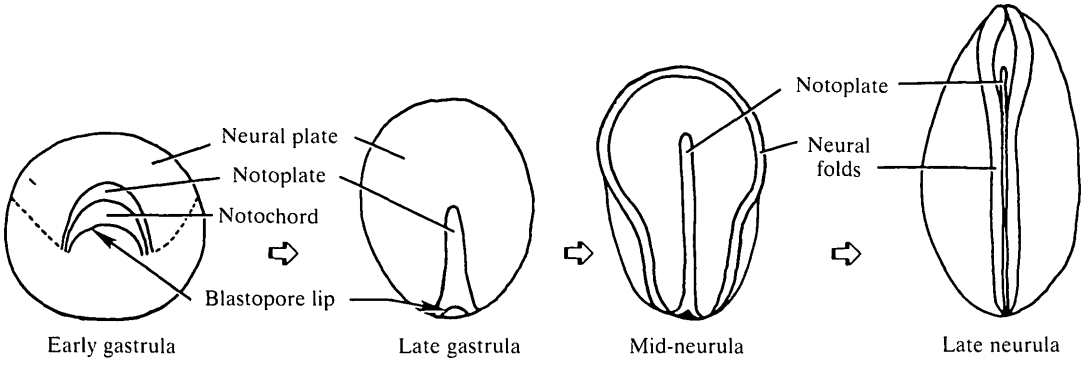

Fig. 5. The parts of the embryo referred to in the text are labelled on these drawings of a rear view of an early gastrula, and dorsal views of late gastrula to late neurula of a newt embryo. The notochord shown above the dorsal lip of the blastopore in the early gastrula has involuted around the blastopore lip, and in subsequent stages lies beneath the notoplate. Figures are approximately to scale. An early gastrula is about 2·5 mm in diameter.

The fate of the floor plate is to become a raphe (i.e. a seam) between the basal plates in the spinal cord and brain. This is precisely the ultimate consequence of the cell behaviour we propose for the notoplate.

The boundary between notoplate and neural plate is an important organizing region for neurulation

Jacobson (1978) found an inverse correlation through time between the length and width of the neural plate of *Taricha torosa*. The implication was that cells were interdigitating themselves so that the plate length increased at the expense of its width. Cell counts of cross sections of the plate reinforced this interpretation. The number of cells in cross sections from a given level of the plate diminished at rates that were inverse to the rate at which the plate elongated.

The boundary between notoplate and neural plate gets progressively longer during neurulation (Fig. 5). The change in the length of this boundary, as measured from time-lapse films of neurulation, was one of the quantitative inputs to the computer simulations of Jacobson & Gordon (1976). They suggested that the boundary elongated as cells from the interior of the notoplate region re-positioned themselves along the boundary.

Adhesive differences between notoplate and neural plate cells are important

Jacobson (1981, 1985) has suggested one means by which this repositioning could come about. He proposed that the adhesive differences between the notoplate cells and the neural plate cells are such that the two cell types should mix, but that the neural plate was more 'solid' than the 'fluid' notoplate area. Thus actual mixing was difficult, and instead the adhesions between notoplate and neural plate cells were maximized by elongating the boundary. For this to happen it would be necessary that the cells move about somehow so that new contacts

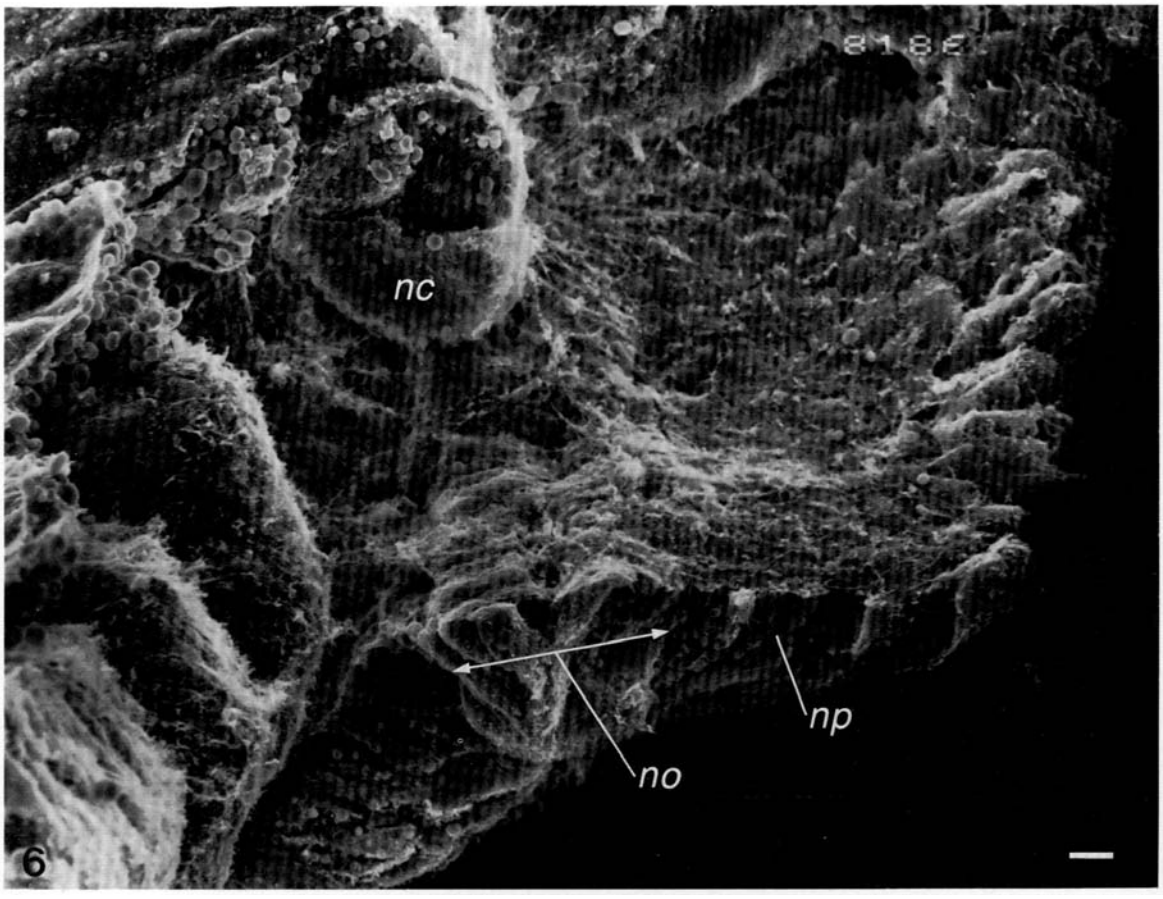

Fig. 6. This scanning electron micrograph shows a view of the bottom and broken face of the neural plate of a *Xenopus laevis* embryo. A piece of the notochord has broken away to reveal the bottoms of the notoplate cells and their relationships to matrix and to the notochord. The notoplate appears distinctly different from the rest of the neural plate in both bottom and edge views. *nc*, notochord; *no*, notoplate; *np*, neural plate. Bar, 10 μm.

would be made between notoplate and neural plate cells. The cortical tractor mechanism provides a means for cells to move about in an epithelium, and in particular a means for active intercalation along the notoplate–neural plate boundary. Coupled with adhesive differences between groups of cells, this endows the boundary between notoplate and neural plate with a central organizing role during neurulation.

The cortical tractor can elongate the notoplate–neural plate boundary

Notoplate cells attach intimately at their basal surfaces to the underlying notochord, while more lateral neural plate cells hang free in the extracellular space where they are probably in contact with extracellular matrix (Fig. 4). Apical

surfaces are normally inactive in epithelia; if contact with the notochord inactivates the basal surfaces of notoplate cells, then notoplate cells can only be active on their lateral faces. Thus one would expect that their cortical tractors would run only laterally. We have examined tangential sections through the notoplate and neural plate and found numerous lateral lamellipodia (Fig. 7), some extending three to four cell ranks away from the cell body. We suggest that these lamellipodia are in fact the organelles which enable the cells to interdigitate between their neighbours by flowing apicalward, as we have described.

The basolateral activity of notoplate cells cannot be random

If the direction of tractoring from the lateral faces were random, then the cells of the notoplate should execute a random walk, and there would be no net distortion of the notoplate in any direction. There are at least two ways that the boundary between the notoplate and the rest of the neural plate could organize the tractoring of the notoplate cells. If notoplate cells that contact neural plate cells adhere to them more strongly than they adhere to each other (differential adhesion), or if contact with a neural plate cell surface inhibits the activity of that face of the notoplate cell (contact inhibition), then tractoring in the notoplate cell will be restricted to those faces not abutting the neural plate. Cells that have just collided often form a new active surface on the face opposite the collision (Trinkaus, 1984*a*, p. 354; Oster, 1984). The result is that cells stuck at the boundary would tractor additional cells toward the boundary, causing them to interdigitate along the boundary and elongate it, as shown in Fig. 8.

Once a notoplate, or neural plate, cell contacts the boundary, it will remain on the boundary thereafter. Some preliminary analyses of time-lapse films of neurulation in *Taricha torosa* support this prediction (Fig. 9). As directed cell interdigitation elongates the notoplate boundary, the adjacent tissues on both sides will be stressed, thus facilitating the interdigitation of further ranks of cells along the axis of the embryo.

We have measured a four-fold increase in the length of the notoplate during neurulation. Interdigitation of just four ranks of cells along the embryonic axis in the notoplate is sufficient to account for this elongation. However, during neurulation there are many more than four ranks of cells in the notoplate, and shortly after neurulation is complete, the descendent of the notoplate, the floor plate, is still four ranks wide at stage 22. The neural tube elongates considerably, and by stage 26, the floor plate is but one cell wide, and that cell is stretched perpendicular to the embryonic axis.

Between stages 13 and 15 the neural plate changes from a disc to a keyhole shape, but the boundary between the edge of the plate and the epidermis remains a constant length (Jacobson & Gordon, 1976). However, at stage 15 this boundary commences to rise and form the neural fold, and the plate begins to roll into a tube. Between stages 15 and 20, as the plate is rolling into a tube, the neural folds elongate by about 30 %. Jacobson & Tam (1982) found that while the brain plate of the mouse embryo rolls into a tube, the neural folds elongate but the midline

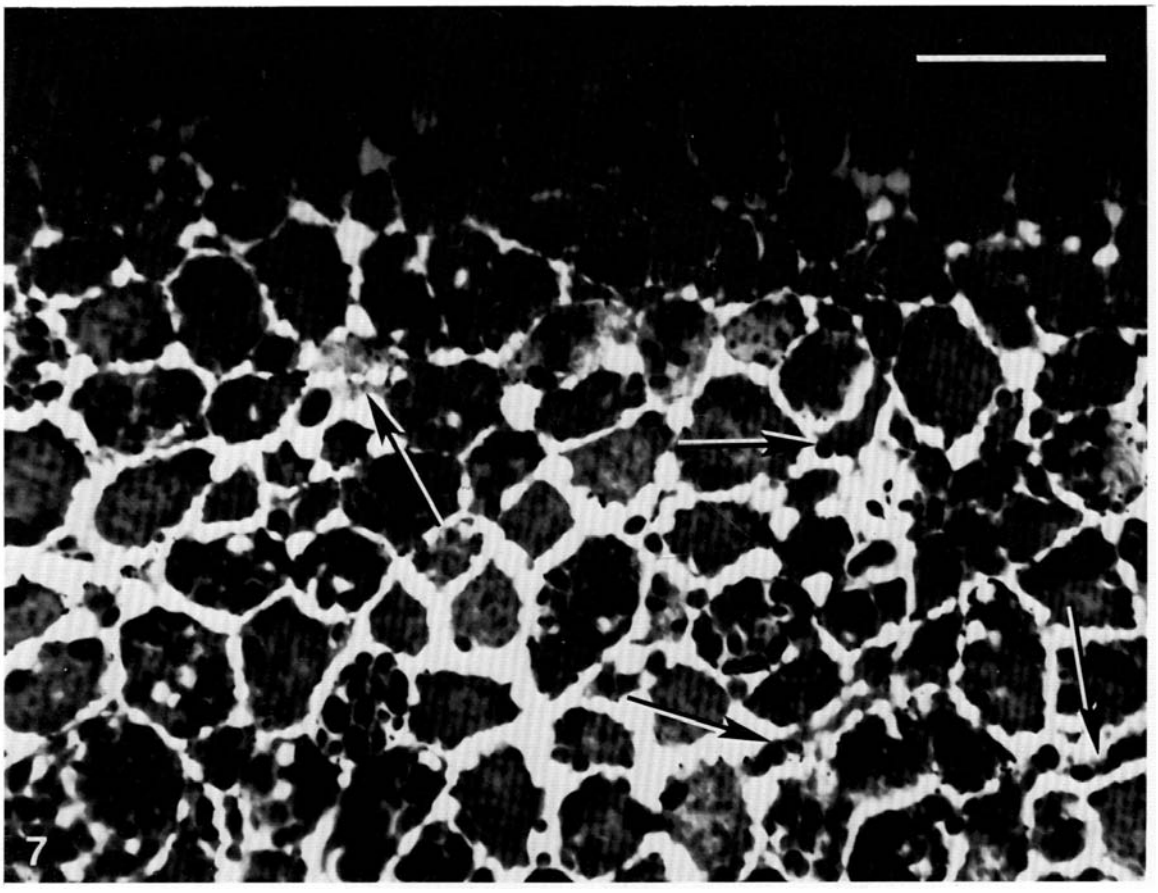

Fig. 7. Tangential, or frontal, section through the neural plate of a stage-17 newt embryo, about halfway down through the thickness of the notoplate. Numerous lamellipodia (arrows) can be seen extending laterally several cell diameters from the bodies of the notoplate cells. The neural plate–notoplate boundary runs across the top of the figure. The plate was removed from underlying tissues (which opened the spaces between the cells somewhat), then fixed immediately in aldehydes, embedded in plastic, and sectioned at 2 μm thickness. Bar, 0·1 mm.

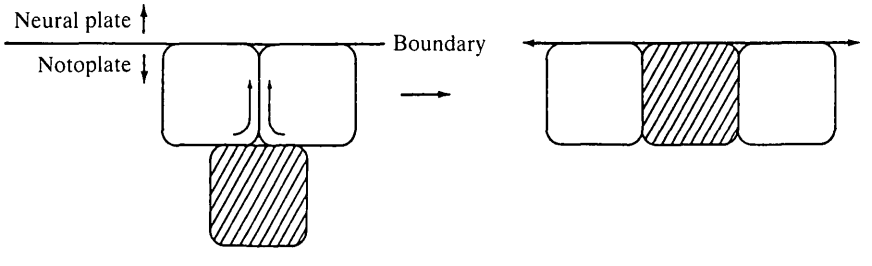

Fig. 8. Schema of how the cortical tractor drives boundary elongation (apical view). The unshaded cells abut the boundary between the notoplate and the neural plate, where their lateral surfaces are deactivated. The other lateral faces continue to tractor as shown, drawing the shaded cell onto the boundary, where it too adheres.

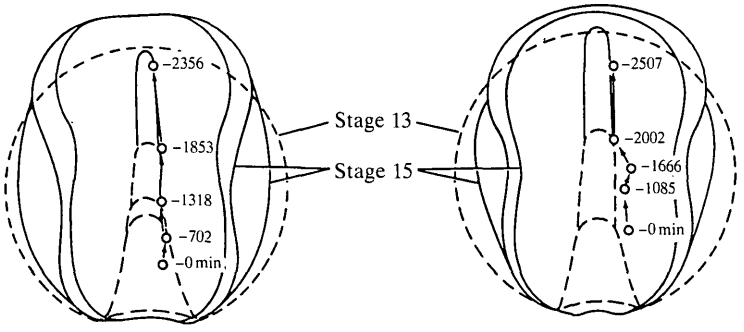

Fig. 9. Cell trajectories have been traced on time-lapse films of early neurulation in the newt embryo. At stage 13 (late gastrula, dashed lines) a cell with distinctive pigmentation was located (labelled 0 min). This cell was followed frame-by-frame, and drawn in at new locations at the intervals indicated. In the figure at the left, the cell was initially within the notoplate area, and had arrived at the notoplate–neural plate boundary by 702 min. (This boundary is drawn in at intervals; it is visible in the film.) Once the cell is on the boundary, it stays there. The solid lines outline the embryo and notoplate at stage 15, when the analysis was terminated. In the figure at the right, a cell that began in the neural plate is similarly traced. This cell arrived at the boundary at 2002 min, and remained there.

does not. The mouse brain plate, which is very wide, also appears to begin rolling near the neural folds. It is evident that the neural fold boundary could also be an organizing line for elongating the neural plate.

The cortical tractor can roll the neural tube while elongating the plate boundary

The cortical tractor model can account for a number of observed cell behaviours at the neural fold boundary. First, we assume that the epidermis is not very active on the basal surface (nor apically, as usual for ectodermal layers). Thus the cells of the epidermis can move only tangentially amongst one another. Second, we assume that the adjacent neural plate cells are basally and laterally active (perhaps because of a different basal environment). As the plate cells tractor, the faces that abut the epidermal cells will adhere to them (or be contact inhibited by them). Since there is a difference in tractor speed between the plate cells and the epidermal cells, the plate cells will crawl beneath the epidermal cells. This crawling will have two consequences.

First, since the apical surfaces of the plate cells are anchored in the epithelial sheet, the cells will be drawn out into long, tapered cells, as shown in Fig. 4 (analogous to bottle-cells in the gastrula). The overlying epidermal cells will be drawn toward the centreline, and a rolling moment will be produced which forces up the plate edge to form the neural fold. (By *rolling moment* we mean a torque generated by a difference in forces between the apical and basal surfaces.) The next rank of plate cells, crawling on the first rank, will commence to elongate and generate a further rolling moment, and so on. This sequence of events is diagrammed in Fig. 10.

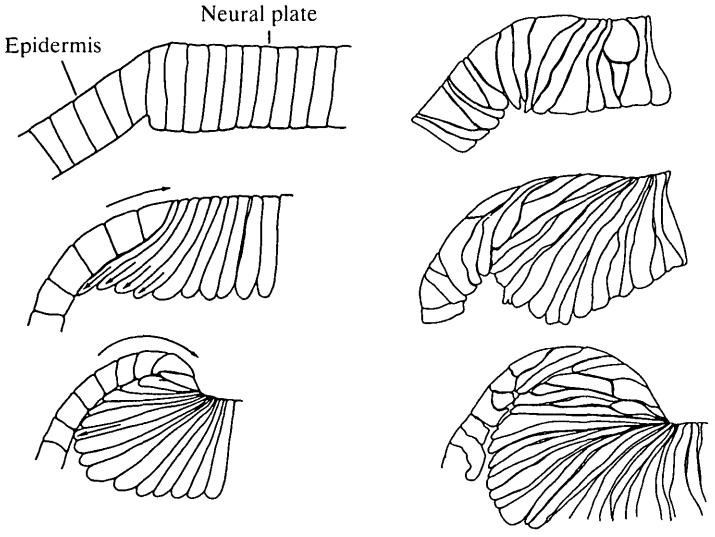

Fig. 10. The diagrams at the left illustrate how we interpret events at the epidermis–neural plate boundary. The drawings on the right are tracings of cells from cross sections of newt neurulae at stages 15, 16, and 17. Because of a difference in tractor velocities, neural plate cells tractor onto the bottoms of the epidermal cells, pulling them into a fold. This stretches the cells until the apical surfaces are attenuated almost to points, or even pull loose from the surface. Neural plate cells also interdigitate along the boundary (interdigitation is not shown in this cross-sectional view) thus lengthening the neural folds. The combination of basal crawling and apical constriction generates a rolling moment that lifts the folds up from the plane of the plate, and rolls toward the midline.

Second, since many ranks of plate cells are crowding onto the boundary region, the boundary will elongate by the same mechanism as the notoplate; that is, epidermal and plate boundary cells contacting one another will have motile activity suppressed at their contacting faces, leaving only those faces away from the boundary active. This effect will spread medially as shown in Fig. 4. Thus differences in tractor intensity between plate and epidermal cells can both elongate the plate boundary, and roll the plate into a tube.

Note that the action of the cortical tractor elongates the cells, and constricts the apical boundary (analogous to the tapering of the tail end of a motile mesenchymal cell which remains attached to the substratum). This has the same mechanical effect as apical contraction *via* circumferential filament bundles, which may also be constricting at this time. The combined effect of apical constriction (*via* tractoring and, or, filament bundles) and basal crawling is to produce a strong rolling moment.

As the plate cells crawl underneath the epidermis, and their apical surfaces constrict, stress is concentrated in the long, thin necks of these bottle-like cells. That is, the traction forces generated by the basal ends will be concentrated in a smaller and smaller apical cross section. Indeed, if the apical ends of the plate cells become sufficiently attenuated, they may accumulate sufficient stress to actually

tear loose from the apical junction structures to form a detached cell population. This may be how neural crest cells separate from the epithelium.

SIMULATION STUDIES OF NEURAL PLATE FOLDING

Neurulation involves the coordination of a number of morphogenetic processes; the three principal cell movements that drive the processes are:

(1) Columnarization of cuboidal cells (i.e. increase in the cell height/cross sectional area ratio) to form the initial neural plate.

(2) Active repacking (i.e. neighbour exchange), especially of notoplate and marginal cells, which elongate the plate centreline and borders.

(3) Generation of bending moments which roll the plate into a tube.

It is not easy to assess the relative importance of the various cellular events listed above. Therefore, we have resorted to computer simulation studies to try and deduce how the various processes contribute and fit together. Here we report some preliminary results based on finite element models developed by Cheng (1986) and Cheng *et al.* (1986), which are described briefly in Appendices A and B.

Columnarization

Odell *et al.* (1981) simulated the neural plate by a finite element model that involved only bending moments generated by apical contraction. They found that, regardless of where the contraction was initiated (e.g. at the centre, or at the plate edges) the first event was the columnarization of the active cells and the flattening of the active cell population into a plate. Cheng (1986) constructed a model for epithelial deformation driven by the cortical tractor mechanism; a brief description is given in Appendix A. This model demonstrates that cell tractoring can also produce columnarization of the plate. Moreover, the model shows how placodes (regions of columnarized cells) arise wherever there is a nonuniformity in tractor velocity. By our third postulate, tractor velocity will vary where there are gradients in ionic environments. This suggests that columnarization may correspond to regions where chemical *gradients* are sustained for some time, perhaps due to altered cell–cell communication *via* gap junctions, or to sources and sinks of chemical 'morphogens'. In the latter case, the cortical tractor 'reads out' its chemical environment in a counterintuitive fashion (cf. Appendix A).

On the basis of the models, therefore, it is only possible to assert that either mechanism, or both mechanisms (tractoring and apical constriction) acting simultaneously and uniformly over the presumptive plate, can produce the initially flattened neural plate. Nor must one conclude that only these two mechanisms are involved in columnarization. For example, Burnside (1971) and others have documented the appearance of vertical arrays of microtubules in columnarized cells, which may play a role in stabilizing the columnar state by 'freezing in' the new cytoskeletal configuration.

Rolling

The simulations of Odell *et al.* (1981) were essentially two-dimensional (i.e. plane stress), and neglected hoop stresses. The finite element model of Cheng lifts these restrictions, but the results, shown in Fig. 11, remain essentially unchanged: bending moments generated either by apical constriction or by tractoring can roll the neural plate into a tube.

Fig. 11 shows the results of applying a uniform rolling moment across the neural plate, due to basal tractoring and/or apical contraction. The sequence of deformed configurations for increasing magnitudes of the applied moment are

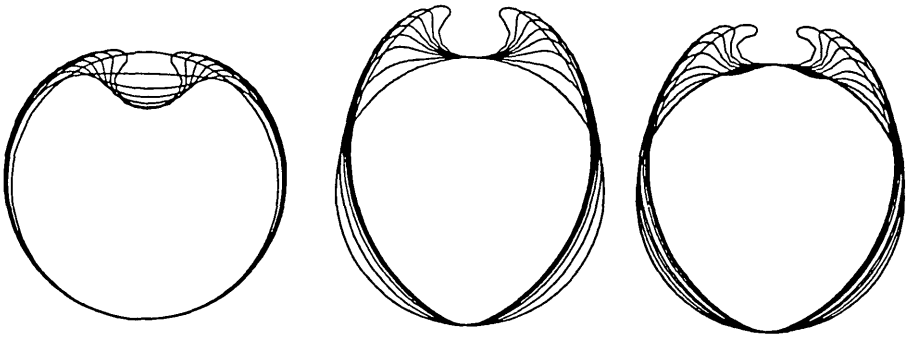

Fig. 11. Computer simulations showing how bending moments generated by the basal crawling of plate cells roll the neural plate model into a tube; see text for discussion.

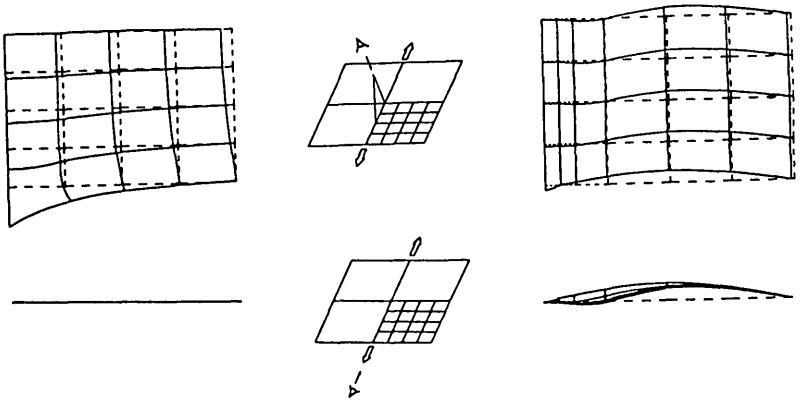

Fig. 12. A pair of forces applied to a plate as shown will produce a transverse buckling force ('Poisson buckling'), as postulated by Jacobson (1981). In this numerical simulation, two forces are applied along a line. If the plate is thick enough (left) it will deform without buckling out of the plane. A thinner plate, however, will buckle up out of its original plane (right). The two views are from the edge (bottom) and from above (top); note that because of the symmetry of the system only a quadrant of the plate is shown. The solid lines show how the undeformed grid (dotted lines) is deformed. The finite element simulation shown here demonstrates that this type of buckling cannot be very large for plates whose thickness to width ratio is more than about 0·1. Thus we conclude that the elongation of the neural plate by active cell interdigitation at the notoplate and the plate edges plays a subordinate role to the buckling moments generated by the cortical tractor and apical constriction.

shown superimposed. These results are qualitatively similar to those of Odell *et al.* (1981), who demonstrated that the rolling moment alone is capable of deforming the neural plate in the proper sequence of shapes: first a flat plate forms, which then rolls into a tube.

The simulations in Fig. 11 also show several other interesting features of neurulation. First, the formation of the plate, and the subsequent rolling of the neural tube, are much more realistically mimicked by the simulations if the notochord is fixed. This suggests a role for the notochord during neurulation as a structural reinforcement supporting the neural plate. Second, the shapes of the neural tube during rolling are much more realistically reproduced if the rolling commences at the plate edge and proceeds inward towards the centreline. This, coupled with the hypothesis that basal crawling of plate cells on the epithelium generate the rolling moment, leads us to conclude that the rolling moment commences at the plate edge, rather than beginning at the centreline, as simulated by Odell *et al.* (1981).

Elongation

Simulations have also demonstrated that pure elongation of the lateral boundary of the neural plate cannot reproduce the proper shape of the neural fold, and cannot roll the plate into a tube unless the plate is unrealistically thin (cf. Fig. 12 and Appendix B). However, in conjunction with the rolling moment, elongation contributes somewhat to the proper shaping of the neural folds. This is in accord with the cortical tractor model, which ascribes both the bending moment and the elongation force to the migration of plate boundary cells underneath the adjacent epithelium and the intercalation of cells at the plate boundary.

The sequence of events during neurulation

We have concluded from the simulations that the sequence that best reproduces the observed shape changes is the following. First, the plate forms by movements that occur over the entire neural plate. These movements produce columnarization of the initially cuboidal plate cells, and can be generated by apical contraction, tractoring, or a combination of the two. Concurrently, elongation of the neural plate occurs first at the centreline and later also at the plate edges. This elongation is driven by the active interdigitation of notoplate cells at the centreline, and the basal crawling and interdigitation of plate cells at the boundary. This elongation is not sufficient by itself to generate much of a rolling moment because of the thickness of the plate: however, it does appear to contribute somewhat to the rolling forces. The elongation also narrows the plate, which facilitates neurulation.

Subsequently, rolling of the neural tube commences at the lateral boundaries of the plate and proceeds inward (rather than from the centre outward, as suggested by the simulations of Odell *et al.* 1981). As we mentioned above, the rolling moments can be generated by apical contraction or tractoring alone, or in combination. However, the configuration of cells shown in Fig. 10 gives strong

support to the supposition that crawling of the marginal cells on the basal epithelium is a strong component of the rolling moment. This is in accordance with our emphasis on the plate–epidermis boundary as an organizing line for neural tube formation. We shall report on more extensive numerical studies in a subsequent publication.

DISCUSSION

Ettensohn has recently reviewed the various proposals for how epithelial sheets invaginate (Ettensohn, 1985). His list of mechanisms includes apical constriction, differential adhesion, cell division and cell rearrangement, amongst others. We have proposed here a new mechanism that can drive epithelial morphogenesis which we call the *cortical tractor model*. This model is built around the notion that the motile behaviour of cells in an epithelial sheet is similar to that of freely migrating mesenchymal cells, with the exception that epithelial cells remain firmly attached at their apical circumference. The term 'cortical tractor' refers to the motion of the cell cortex: cytogel flows in a fountainoid whose source is near the basal cortex, and whose sink is on or near the apical surface.

The model presumes that membrane and cell adhesive structures are inserted at a basal source, flow apicalward, and are eventually recycled to the cell interior at an apical sink. Junctional structures pile up at the apical periphery because resorption cannot keep up with the insertion rate.

According to the cortical tractor model, the motive force for epithelial morphogenesis derives from the motile activity of the basal and, or, lateral surfaces of the cells. Thus basal crawling generates shear forces on the lateral surfaces between cells, and constricts the apical surface. This is not exclusive of apical constriction by circumferential filament bundles; indeed, the tractor motion can provide the mechanism that accumulates actomyosin structures in the apical region.

Thus the cortical tractor model shifts the focus of attention from the apical surface to the basal and lateral surfaces where motile activity is hidden from direct observation. Indeed, micrographic examination of these surfaces in active epithelia does reveal an abundance of protrusive lamellae and filopodia. The time-averaged motions of these protrusions create the fountainoid flow, and provide the motive force driving epithelial deformations by several mechanisms.

First, the tractor motion can generate shear forces between cells whose cortical velocities differ. These shear forces tend to columnarize the cells, a phenomenon that usually precedes epithelial folding (Ettensohn, 1985).

Second, if the basal surface can attach to a substratum – for example, an adjacent cell whose tractor speed is slower – then the tractions it develops can generate a bending moment. Furthermore, the constriction of the apical surface associated with the tractor motion contributes to this bending moment.

Finally, the cortical motion that sweeps junctional structures apicalward provides a mechanism by which epithelial cells can interdigitate between one another,

changing their neighbours and repacking the sheet without violating the integrity of the apical seal. Active cell rearrangement appears to drive many epithelial deformations, and the cortical tractor model provides an explanation for how that process can come about.

In the absence of direct *in vivo* observations, we have attempted to provide evidence in favour of the cortical tractor model *via* three routes. First, by examining micrographs of the basal and lateral surfaces of epithelia known to be engaged in morphogenetic activity, we find an abundance of motile appendages. Second, we have examined the mechanical consequences of the cortical tractor motion using mathematical analysis and computer simulations. We find that the postulated tractor motion can indeed generate the required forces and bending moments to produce realistic-looking epithelial foldings. We have used the neural plate as an example here, where we predicted that cells in the notoplate, or in the neural plate, would move about randomly by tractoring until they interdigitated at the notoplate–neural plate boundary, where they should remain. Our observations from time-lapse films confirmed this prediction. Finally, the cortical tractor model is consistent with a wide range of observations on epithelial morphogenesis (cf. Ettensohn, 1985).

Indeed, the cortical tractor model provides the mechanical apparatus necessary to implement the various other hypotheses of epithelial morphogenesis, including apical constriction, active repacking and adhesive disparity. For example, the adhesive disparity models of Gustafson & Wolpert (1962, 1967), Mittenthal & Mazo (1983) and others suggest that cell adhesion differences can drive epithelial invagination. However, adhesive forces cannot by themselves drive cell motions, for adhesion is a force normal to the cell surface. A tangential force is required in order to bring surfaces with different adhesive strengths into contact. The cortical tractor motion provides the tangential (i.e. shear) forces required to translocate cell surfaces relative to their surroundings. Moreover, the insertion of membrane and adhesive structures at the basal source and their subsequent apical flow and reingestion provides the mechanism for creating and modulating the surface adhesion properties of each cell. Thus the cortical tractor model does not replace the notion of adhesive disparity, but provides the mechanical mechanism for implementing differential adhesion as a morphogenetic mechanism.

We do not imagine that the cortical tractor model will provide an explanation for all epithelial morphogenesis. Indeed, we agree with Ettensohn's (1985) conclusion that different mechanisms may predominate in different settings. However, we feel that by drawing attention away from the apical surface, so visible and compelling, and focusing on the basal and lateral surfaces, which manifest so much motile activity, the cortical tractor model can at least provide a new focus for investigating epithelial morphogenesis.

This work was supported by grants NS 16072 from NIH to A.G.J., by NSF Grant MCS-8110557 to G.F.O. and L.Y.C. and by NSF Grant No. MCS-8301460 to G.M.O. We would like to thank

Raymond Keller for valuable discussions, and James D. Murray who collaborated with us in deriving the placode equations.

APPENDICES

(A) *The cortical tractor model for epithelial columnarization*

In this Appendix we sketch the basic equations that govern a cortical tractor model for epithelial deformations (cf. Cheng *et al.* 1986). The complete equations for the cortical tractor model are quite complex. However, by restricting attention to the vertical force components we can easily write the equations governing the formation of placodes, regions of columnar cells whose formation always precedes further folding or invaginations.

(1) *Finite difference equations for normal displacements*

The simplest model for the cortical tractor can be derived by considering the free body diagram in Fig. 13. Here we represent two adjacent cells by trapezoidal elements, whose vertices are denoted by $(i-1, i, i+1)$, and refer to the cell with boundaries i, $i+1$ as cell i. We shall employ the following notation:

H_i = the height at node i (i.e. the boundary between cell i and cell $i-1$)
H_o = the initial (unstressed) height of each cell
$\lambda_i = H_i/H_o$ = the stretch ratio at node i
W_i = the width of cell i
W_o = the initial (unstressed) width of each cell
v_i = the velocity of the cortical flow in cell i
k = the elastic modulus of each cell
G = the passive shear modulus of each cell

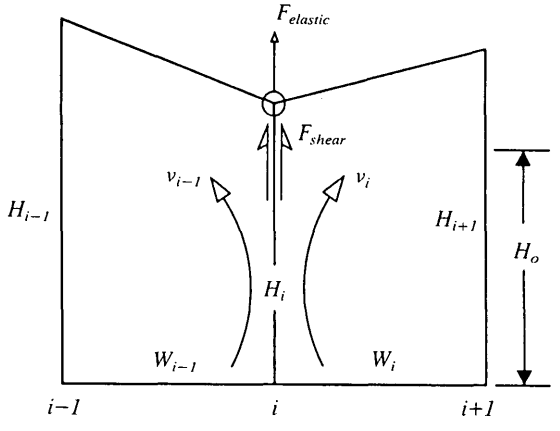

Fig. 13. A free body diagram of two adjacent cells showing the elastic, shear and tractor forces acting on node i (From Cheng, Murray, Odell & Oster, 1986).

α = the active shear modulus for each cell due to tractor motion
μ = viscosity of the cortical cytoplasm

The equations for motion for cell i are derived by writing down force balance equations on node i for the vertical force components; i.e. by equating the sum of the forces to the intertial force, md^2H_i/dt^2, where m is the mass of a cell. However, for this system the inertial forces are negligible (Odell *et al.* 1981), so that we need not consider the acceleration term on node i. Thus the force balance equation for node i is:

$$F_{ELASTIC} + F_{SHEAR} + F_{ACTIVE} + F_{VISCOUS} = 0 \tag{1}$$

which can be approximated by

$$\underbrace{\mu \frac{dH_i}{dt}}_{\text{VISCOUS FORCES}} = -k \underbrace{\left[\left(\frac{H_i + H_{i+1}}{2} - H_o\right)\frac{W_i}{2} + \left(\frac{H_{i-1} + H_i}{2} - H_o\right)\frac{W_{i-1}}{2}\right]}_{\text{PASSIVE ELASTIC FORCES}} \tag{2}$$

$$- G \underbrace{\left[\left(\frac{H_i - H_{i-1}}{2}\right) + \left(\frac{H_i - H_{i+1}}{2}\right)\right]}_{\text{PASSIVE SHEAR ELASTIC FORCES}} + \underbrace{\alpha[(v_i - v_{i-1})\, H_i]}_{\text{ACTIVE SHEAR FORCES}}$$

where k is an elastic modulus and G a shear modulus. Here forces tending to shorten the cell are counted as negative. Note that, in the elastic force term, the terms in parentheses are the elastic forces per unit width of a cell, multiplied by the half-width of the cell. This assigns half the elastic force generated by each cell to a node. The active shear force modulus, α, is per unit height, and so is multiplied by the cell height, H_i. Note also that the shear forces depend on the absolute value of the tractor velocity differences between cells, since only relative motion is required to produce active shears.

Since cytoplasm is incompressible, we shall also impose an incompressibility constraint on each cell:

$$\left(\frac{H_i + H_{i+1}}{2}\right) W_i = H_o W_o \tag{3}$$

Thus we can eliminate W_i from the above equations and, after dividing through by H_o, the equations of motion can be written in terms of the strain, λ_i, only.

These equations may be simulated directly as finite difference equations, and we shall present an extensive study elsewhere (see Cheng *et al.* 1986). Two examples of the counterintuitive properties of the cortical tractor will be discussed below.

(2) *Field equations*

Some insight into the behaviour of the model can be gleaned by converting the above equations into a continuum model. There is no unique correspondence between the above finite difference equations and a set of partial differential

equations. However, we can proceed in the most elementary fashion by the following identifications:

$$\lambda_i \longrightarrow \lambda(x,t),\ x_{i+1} - x_i \longrightarrow \delta$$

so that we can expand λ in a Taylor's series to second order, e.g.

$$\lambda_{i+1} \longrightarrow \lambda(x) + \delta\frac{\partial\lambda}{\partial x} + \frac{\delta^2}{2}\frac{\partial^2\lambda}{\partial x^2} + \cdots$$

This yields the following nonlinear partial differential equation for $\lambda(x,t)$:

$$\mu\frac{\partial\lambda}{\partial t} = -K_o\left(1-\frac{1}{\lambda}\right) - \frac{K_1}{\lambda^3}\left(\lambda\frac{\partial^2\lambda}{\partial x^2} - \left(\frac{\partial\lambda}{\partial x}\right)^2\right) + G_1\frac{\partial^2\lambda}{\partial x^2} + \lambda\left|\alpha_o\lambda\frac{\partial v}{\partial x} - \alpha_1\lambda\frac{\partial^2 v}{\partial x^2}\right| \quad (4)$$

where we have employed the constant volume constraint and defined the following quantities:

$$\begin{aligned} K_o &= kW_o \\ K_1 &= \tfrac{1}{4}kW_o\delta^2 \\ G &= \tfrac{1}{2}G\delta^2 \\ \alpha_o &= \alpha\delta \\ \alpha_1 &= \tfrac{1}{2}\alpha\delta^2 \end{aligned}$$

The linearized version of equation (4) is easier to understand and captures the essential features. Therefore we can substitute $\lambda = 1+u$ into the above equation and retain only linear terms in u, the height perturbation. Thus for small velocity perturbations, $v(x)$, the linearized cortical tractor model is:

$$\mu\frac{\partial u}{\partial t} = -K_o u + D\frac{\partial^2 u}{\partial x^2} + \left|\alpha_o\frac{\partial v}{\partial x} - \alpha_1\frac{\partial^2 v}{\partial x^2}\right| . \quad (5)$$

where $D = G_1 - K_1$.

The first term on the right-hand side of this equation is the passive elastic force tending to restore the cells to their unstrained cuboidal shape. The second term is the elastic forces tending to smooth out variations in cell height. If $G > kW_o/2$ this term is always stabilizing; however, if $G < kW_o/2$ the system may become numerically unstable under perturbations whose wavelength is shorter than the width, W_o, of the finite element. This is simply an artifact of the continuum limit: physically, the passive elastic forces cannot generate deformations. The third and fourth terms arise from the active shearing stresses generated by the cortical tractor. The third term is an active 'convection-like' force which tends to deform the sheet wherever there is a *gradient* in tractor velocity, v. The fourth term is the active shearing force which tends to amplify height variations.

Note that because of the incompressibility constraint, the taller a cell grows, the narrower it becomes. Therefore, the strain λ is proportional to the cell density. Therefore, we can substitute for u the normalized cell density deviation

$(N-N_o)/N_o$, where N_o is the undeformed cell density (i.e. when $\lambda = 1$, $u = 0$), and obtain an equation in cell density, N, which has the same form as equation (5).

If a cortical tractor velocity, v, is prescribed by some means (e.g. a boundary condition, or a chemical gradient) then equation (4) predicts a variation in cell density, and therefore in cell shape, wherever variations in v arise. This is because the active shear forces which tend to deform the cells can only arise when *gradients* in v are present. The consequences of this simple mechanical effect are quite subtle, as discussed in detail by Odell & Bonner (1986) where a similar model was applied to the morphogenesis of slime moulds. In the present setting, it is worth noticing that a constant linear gradient in the tractor velocity, v, produces a uniform placode ($u > 0$), as shown in Fig. 14A. Furthermore, an asymmetric velocity profile (e.g. $u \propto sin(x)$) produces an asymmetric deformation which is displaced, as shown in Fig. 14B. Since local chemical conditions regulate the

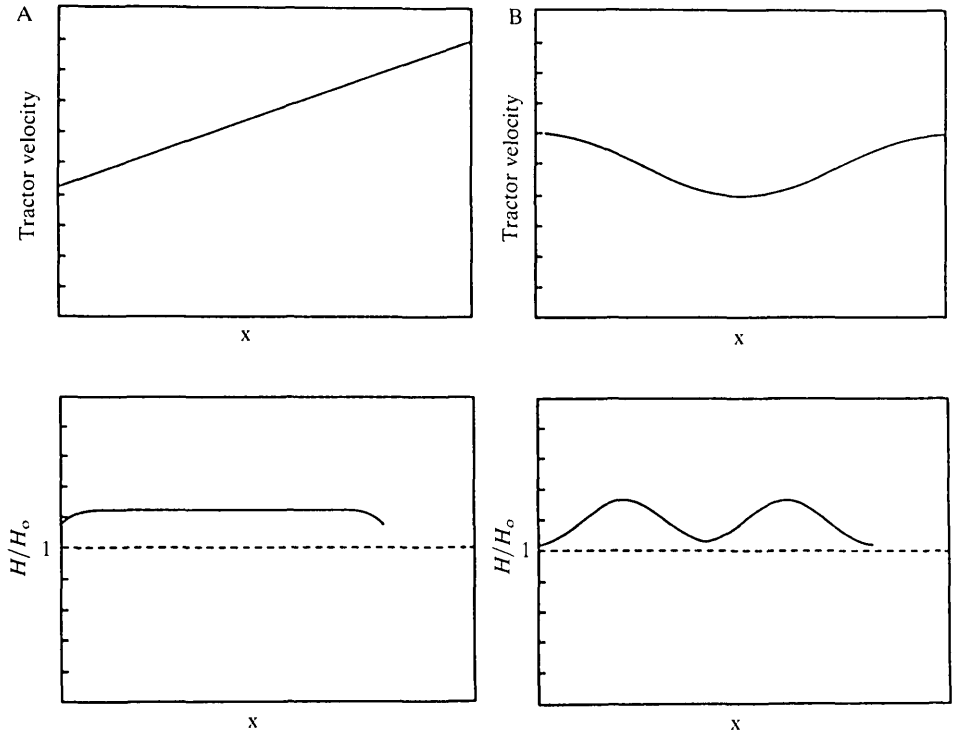

Fig. 14. The deformation fields corresponding to two simple tractor velocity fields. The tractor velocity is a monotone function of local chemical conditions, and so the variation in $v(x)$ can be taken as reflecting the spatial chemical concentration distribution. (A) A uniform gradient in tractor velocity, v, produces a placode of constant height: i.e. a constant displacement field $u(x)$, where x measures distance along the cell sheet and u measures the height perturbation from the uniform, unperturbed state. The taper at the edges is due to the imposition of zero displacement boundary conditions. (B) A periodic tractor velocity field, $v(x)$, produces a displacement field, $u(x)$ which is shifted with respect to the velocity field (from Cheng, Murray, Odell & Oster, 1986).

tractor velocity, v, this implies that the cortical tractor 'reads out' chemical conditions in a somewhat counterintuitive fashion.

(B) *The finite element shell model of the neural plate*

The finite element method

The simulations of neural folding shown in Figs 11 and 12 were performed using a finite element model for shell-like bodies (Zienkiewicz, 1977). This method is based on a variational formulation, which minimizes a functional representing the total energy of the mechanical system. A material body is first subdivided into a collection of sub-bodies, each of which is modelled by a finite element that represents its geometric and mechanical characteristics. One then computes the contributions to the energy functional from all of the elements, and then minimizes this functional to obtain the geometric configuration of the complete body. No restrictions need be placed on the shapes and mechanical properties of the elements, and so systems with complicated geometry and physical properties may be analysed.

In order to formulate the energy functional which characterizes the system, one must account for three kinds of relationships:

(1) The equations of mechanical equilibrium. These relate the external forces applied to the system to the pattern of internal stresses.

(2) The kinematic relationships, which relate the strains within the material to the displacement of material points of the body.

(3) The constitutive relation which specifies the mechanical properties of the material by a stress–strain equation.

In applying the finite element method to the neural plate, we have specialized to the case of thin-shelled bodies. This is because the thickness of the neural plate is rather small compared to the plate radius (i.e. a thickness/radius ratio of less than 10 is sufficient).

The neural plate model

We have studied several possible mechanisms of neural plate deformation separately in order to assess their relative contributions to the observed morphological changes. The combined effects of apical constriction (*via* apical filament bundle contraction and, or, tractoring) and basal crawling is to produce a rolling moment. Elongation of the notoplate can also induce a rolling moment by generating a transverse compression ('Poisson buckling'). First, we study the pure rolling problem employing the axisymmetric shell elements developed by Cheng (1986). The curved plate geometry was achieved by modelling the embryo as a torus, with a very large major radius. The thickness/radius ratio was taken as 1/10 for the epidermal cell layer, and twice that for the neural plate. These represent the approximate size proportions at the time of tube formation. Although the effects of apical constriction and basal crawling both create an active rolling moment, they were modelled in different ways. The effect of apical constriction

was imposed over the entire plate simultaneously, whereas basal crawling initiated near the plate margin (cf. Fig. 10), and progressed toward the midline, since this pattern of moments produced the most realistic sequence of plate geometries.

In order to investigate the role of midline and, or, marginal elongation a full three-dimensional model is required. We employed for this a general purpose finite element program called ABAQUS (Hibbit, Karlsson & Sorensen, 1982). The neural plate was modelled as flat plate, as shown in Fig. 12.

A tangential force was applied to the plate along the midline to produce the elongation. A small perturbation in the vertical direction (modelled as a uniformly distributed vertical pressure) was introduced to initiate the buckling instability. Plate thicknesses around 1/20 and 1/200 were employed, and the simulations showed that Poisson buckling was only significant for quite thin plates.

In the above analyses, the elastic properties of the epithelial cells was represented by a Hookian (linear) constitutive relation, and viscous effects were ignored. In all cases the formulations we used were valid for large displacements. A complete description of the simulations will be published elsewhere.

REFERENCES

ABERCROMBIE, M. (1980). The crawling movement of metazoan cells. *Proc. R. Soc.* B **207**, 129–147.

ABERCROMBIE, M., HEAYSMAN, J. E. M. & PEGRUM, S. M. (1970). The locomotion of fibroblasts in culture. III. Movements of particles on the dorsal surface of the leading lamella. *Expl Cell Res.* **62**, 389–398.

ALLEN, R. D. (1961). A new theory of amoeboid movement and protoplasmic streaming. *Expl Cell Res.* **8 (Suppl.)**, 17–31.

BAKER, P. C. & SCHROEDER, T. E. (1967). Cytoplasmic filaments and morphogenetic movement in the amphibian neural plate. *Devl Biol.* **15**, 432–450.

BRETSCHER, M. S. (1984). Endocytosis: Relation to capping and cell locomotion. *Science* **224**, 681–686.

BURNSIDE, B. (1971). Microtubules and microfilaments in newt neurulation. *Devl Biol.* **85**, 416–441.

BURNSIDE, B. (1973). Microtubules and microfilaments in amphibian neurulation. *Am. Zool.* **13**, 989–1006.

BURNSIDE, M. B. & JACOBSON, A. G. (1968). Analysis of morphogenetic movements in the neural plate of the newt *Taricha torosa. Devl Biol.* **18**, 537–552.

CAMPBELL, R. D. & CAMPBELL, J. H. (1971). Origin and continuity of desmosomes. In *Results and Problems in Cell Differentiation*, vol. 2, *Origin and Continuity of Cell Organelles* (ed. J. Reinhert & H. Ursprung), pp. 261–298.

CHENG, L. Y. (1986). Applications of mechanics to cell and developmental biology. Report No. UCB/SESM-86/01, Civil Engineering Department, University of California, Berkeley.

CHENG, L. Y., MURRAY, J., ODELL, G. M. & OSTER, G. F. (1986). The cortical tractor: a new model for epithelial morphogenesis. In *Lecture Notes in Biomathematics*. Berlin: Springer-Verlag (in press).

COOPER, M. & SCHLIWA, M. (1985). Electrical and ionic controls of tissue cell locomotion in DC electric fields. *J. Neurosci. Res.* **13**, 223–244.

DEMBO, M. & HARRIS, A. K. (1981). Motion of particles adhering to the leading lamellae of crawling cells. *J. Cell Biol.* **91**, 528–536.

DOWNIE, J. R. & PEGRUM, S. M. (1971). Organization of the chick blastoderm edge. *J. Embryol. exp. Morph.* **26**, 623–635.

ETTENSOHN, C. A. (1985). Mechanisms of epithelial invagination. *Q. Rev. Biol.* **60**, 289–307.

FRISTROM, D. K. (1982). Septate junctions in imaginal discs of *Drosophila*: A model for the redistribution of septa during cell rearrangement. *J. Cell Biol.* **94**, 77–87.

GERHART, J. C. (1980). Mechanisms regulating pattern formation in the amphibian egg and early embryo. In *Biological Regulation and Development* (ed. R. F. Goldberger), pp. 133–293. New York: Plenum.

GUSTAFSON, T. & WOLPERT, L. (1962). Cellular mechanisms in the morphogenesis of the sea urchin larva. Change in shape of cell sheets. *Expl Cell Res.* **27**, 269–279.

GUSTAFSON, T. & WOLPERT, L. (1967). Cellular movement and contact in sea urchin morphogenesis. *Biol. Rev. Camb. Phil. Soc.* **42**, 442–498.

HARDIN, J. & CHENG, L. Y. (1986). The mechanisms and mechanics of archenteron elongation during sea urchin gastrulation. *Devl Biol.* (in press).

HARRIS, A. K. (1973). Cell surface movements related to cell locomotion. In *Locomotion of Tissue Cells, Ciba Foundation Symposium* **14** (new series) (ed. R. Porter & D. W. Fitzsimons), pp. 3–26. Amsterdam: Elsevier/North Holland.

HARRIS, A. K. & DUNN, G. (1972). Centripetal transport of attached particles on both surfaces of moving fibroblasts. *Expl Cell. Res.* **73**, 519–523.

HAY, E. D. (1968). Organization and fine structure of epithelium and mesenchyme in the developing chick embryo. In *Epithelial–Mesenchymal Interactions* (ed. R. Fleischmajer & R. E. Billingham), pp. 31–55. Baltimore: Williams & Wilkins Co.

HIBBIT, KARLSSON & SORENSEN, INC. (1982). ABAQUS Users' Manual. 35 South Angeli Street, Providence RI 02906.

HITCHCOCK, S. E. (1977). Regulation of motility in non-muscle cells. *J. Cell Biol.* **74**, 1–15.

HOLTFRETER, J. (1946). Structure, motility and locomotion in isolated embryonic amphibian cells. *J. Morph.* **79**, 27–62.

HOLTFRETER, J. (1947). Changes of structure and the kinetics of differentiating embryonic cells. *J. Morph.* **80**, 57–92.

JACOBSON, A. G. (1978). Some forces that shape the nervous system. *Zoon* **6**, 13–21.

JACOBSON, A. G. (1981). Morphogenesis of the neural plate and tube. In *Morphogenesis and Pattern Formation* (ed. T. G. Connelly, L. L. Brinkley & B. M. Carlson), pp. 233–263. New York: Raven Press.

JACOBSON, A. G. (1985). Adhesion and movement of cells may be coupled to produce neurulation. In *The Cell in Contact: Adhesions and Junctions as Morphogenetic Determinants* (ed. G. M. Edelman & J.-P. Thiery), pp. 49–65. New York: John Wiley and Sons.

JACOBSON, A. G. & GORDON, R. (1976). Changes in the shape of the developing nervous system analysed experimentally, mathematically, and by computer simulation. *J. exp. Zool.* **197**, 191–246.

JACOBSON, A. G., ODELL, G. M. & OSTER, G. F. (1985). The cortical tractor model for epithelial folding: Application to the neural plate. In *Molecular Determinants of Animal Form, UCLA Symposia on Molecular and Cellular Biology* (new series), vol. 31 (ed. G. M. Edelman), pp. 143–167. New York: Alan R. Liss, Inc.

JACOBSON, A. G. & TAM, P. P. L. (1982). Cephalic neurulation in the mouse embryo analysed by SEM and morphometry. *Anat. Rec.* **203**, 375–396.

KELLER, R. E. (1978). Time-lapse cinemicrographic analysis of superficial cell behavior during and prior to gastrulation in *Xenopus laevis*. *J. Morph.* **157**, 223–248.

KELLER, R. E., DANILCHIK, M., GIMLICH, R. & SHIH, J. (1985). Convergent extension by cell intercalation during gastrulation of *Xenopus laevis*. In *Molecular Determinants of Animal Form, UCLA Symposium on Molecular and Cellular Biology* (new series), vol. 31 (ed. G. M. Edelman), pp. 111–142. New York: Alan R. Liss, Inc.

LARSEN, W. & RISINGER, M. (1985). The dynamic life histories of intercellular junctions. In *Modern Cell Biology*, vol. 4 (ed. B. Satir). New York: Alan R. Liss.

MEIER, S. (1984). Somite formation and its relationship to metameric patterning of the mesoderm. *Cell Differ.* **14**, 235–243.

MIDDLETON, C. A. (1973). The control of epithelial cell locomotion in tissue culture. In *Locomotion of Tissue Cells, Ciba Foundation Symposium* **14** (new series) (ed. R. Porter & D. W. Fitzsimons), pp. 251–269. Amsterdam: Elsevier/North Holland.

MITTENTHAL, J. & MAZO, R. (1983). A model for shape generation by strain and cell–cell adhesion in the epithelium of an arthropod leg segment. *J. theor. Biol.* **100**, 443–483.

NEW, D. A. T. (1959). Adhesive properties and expansion of the chick blastoderm. *J. Embryol. exp. Morph.* **7**, 146–164.

ODELL, G. M. & BONNER, J. T. (1986). How the *Dictyostelium discoideum* grex crawls. *Phil. Trans. R. Soc. Lond.* (in press).

ODELL, G. M. & FRISCH, H. L. (1975). A continuum theory of the mechanics of amoeboid pseudopodium extension. *J. theor. Biol.* **50**, 59–86.

ODELL, G. M., OSTER, G., ALBERCH, P. & BURNSIDE, B. (1981). The mechanical basis of morphogenesis. I. Epithelial folding and invagination. *Devl Biol.* **85**, 446–462.

OSTER, G. F. (1984). On the crawling of cells. *J. Embryol. exp. Morph.* **83**, **Suppl.**, 329–364.

PETRIS, S. DE & RAFF, M. C. (1973). Fluidity of the plasma membrane and its implications for cell movement. In *Locomotion of Tissue Cells, Ciba Foundation Symposium* **14** (new series) (ed. R. Porter & D. W. Fitzsimons), pp. 27–52. Amsterdam: Elsevier/North Holland.

RADICE, G. P. (1980*a*). The spreading of epithelial cells during wound closure in *Xenopus* larvae. *Devl Biol.* **76**, 26–46.

RADICE, G. P. (1980*b*). Locomotion and substratum contacts of *Xenopus* epidermal cells *in vitro* and *in situ*. *J. Cell Sci.* **44**, 201–223.

RUGH, R. (1948). *Experimental Embryology*, p. 101. Minneapolis: Burgess Publishing Co.

SCHOENWOLF, G. C. (1985). Shaping and bending of the avian neuroepithelium: Morphometric analysis. *Devl Biol.* **109**, 127–139.

SNYDERMAN, R. & GOETZL, E. (1981). Molecular and cellular mechanisms of leukocyte chemotaxis. *Science* **213**, 830–837.

SPEMANN, H. (1938). *Embryonic Development and Induction*, 401 pp. New Haven: Yale University Press.

SPEMANN, H. & MANGOLD, H. (1924). Über Induktion von Embryonalanlagen durch Implantation artfremder Organisatoren. *Wilhelm Roux Arch. EntwMech. Org.* **100**, 599–638.

TRINKAUS, J. P. (1984*a*). *Cells into Organs. The Forces that Shape the Embryo*, 2nd edn, 543 pp. Englewood Cliffs, NJ: Prentice-Hall.

TRINKAUS, J. P. (1984*b*). Mechanism of Fundulus epiboly – A current view. *Amer. Zool.* **24**, 673–688.

VAUGHN, R. B. & TRINKAUS, J. P. (1966). Movements of epithelial cell sheets *in vitro*. *J. Cell Sci.* **1**, 407–413.

ZIENKIEWICZ, O. C. (1977). *The Finite Element Method*, 3rd edn. London: McGraw-Hill.

ZIGMOND, S. (1978). Chemotaxis by polymorphonuclear leukocytes. *J. Cell Biol.* **77**, 269–287.

(*Accepted 1 April 1986*)